Nov 8th, 12:00 AM

Distortional Buckling Tests of Cold-formed Channel Sections

Gregory J. Hancock

Sammy C. W. Lau

Ninth International Specialty Conference on Cold-Formed Steel Structures
St. Louis, Missouri, U.S.A., November 8-9, 1988

DISTORTIONAL BUCKLING TESTS OF COLD-FORMED CHANNEL SECTIONS

Sammy C.W. Lau[1] and Gregory J. Hancock[2]

Summary

The results of compression tests of thin-walled channel section columns formed by brake-pressing are described. A total of 68 channel section columns of different section geometries, thicknesses and steel grades were tested under uniform compression in fix-ended condition. The length of the columns ranged from short length stub columns which failed mainly by inelastic local buckling, to intermediate length columns which failed by inelastic distortional buckling to long length columns which failed by either elastic or inelastic flexural-torsional buckling. Design curves to account for the inelastic behaviour in the distortional mode of buckling are proposed in the paper and compared with the test results. The test results are also compared with the recently revised Australian Standard, American Specification and European Recommendations for the design of cold-formed steel structures.

1 Postgraduate Student, School of Civil and Mining Engineering, University of Sydney, Australia, 2006

2 Associate Professor, School of Civil and Mining Engineering, University of Sydney, Australia, 2006

1. INTRODUCTION

The columns of industrial steel storage rack structures are generally cold-formed open sections manufactured either by roll-forming or brake-pressing. The commonly used sections are thin-walled lipped channels whose width and depth are approximately equal. Depending on the length of the columns and the restraints provided by the pallet beams and bracing, these types of sections may fail in the modes of local, distortional or flexural-torsional buckling. In a recent paper by Hancock (1985), it was shown both theoretically and experimentally that the distortional mode of buckling may govern the design for columns of intermediate slenderness. Subsequently, an approximate analytical expression was derived by Lau and Hancock (1987) for calculating the elastic critical stress of distortional buckling for channel sections under uniform compression. The purpose of this paper is to provide further experimental results on the distortional buckling mode for a variety of channel section columns in order to calibrate a column design curve both in the elastic and inelastic range of buckling.

The theoretical and experimental work presented in Hancock (1985) and Lau and Hancock (1987) dealt with the distortional buckling mode where the critical stress is within the elastic range. Unlike hot-rolled steel sections which usually have a sharp yielding stress-strain curve for the material making up the sections, cold-formed steel sections may have a rounded stress-strain curve when approaching the yield stress. The nonlinear range of the stress-strain curve is important for columns of intermediate slenderness which buckle inelastically. Consequently, the inelastic distortional buckling stress will depend upon the stress-strain characteristics of the steel making up the sections. These characteristics are reported for both tensile and compression coupons taken from the test specimen material.

In this paper, the results of compression tests of thin-walled steel channel section columns formed by brake-pressing are described. A total of 68 channel columns of different section geometries, thicknesses and steel grades were tested under uniform compression with the ends being fixed. The length of the test columns ranged from short stub columns to intermediate length columns which failed by inelastic distortional buckling to long length columns which failed by either elastic or inelastic flexural-torsional buckling. A design curve to account for the interaction of yielding and buckling in the distortional mode is proposed in the paper. A design method (called 'Australian Alternative II') based on this curve is proposed in the paper. The test results are also compared with the recently revised Australian Standard (1988) (called 'Australian Alternative I'), European Recommendations (1987) and the AISI Specification (1986) for the design of cold-formed steel structures.

2. DISTORTIONAL BUCKLING MODE OF CHANNEL SECTION COLUMNS

A detailed description of the buckling modes of channel sections subjected to uniform compression can be found in Hancock (1985). The distortional mode, as shown in Fig. 1, involves a rotation of the flange and lip combinations about the flange/web junctions, with the web element (called the 'front face' in rack columns) restraining the flanges. The degree of restraint provided by the web depends upon the slenderness of the web and the degree to which it is also destabilised by the compressive stress in the section. This buckling mode has been referred as local-torsional in some reports.

3. TEST SECTIONS

Four types of channel columns of different section geometries were chosen for testing. The shapes of the channel sections chosen were similar to those studied in Lau and Hancock (1987). They were the simple lipped channels as shown in Fig. 2(a) (designated 'CH'), the rack column uprights as shown in Fig. 2(b) (designated 'RA'), the rack column uprights with additional lip stiffeners as shown in Fig. 2(c) (designated 'RL') and the hat sections as shown in Fig. 2(d) (designated 'HA'). The finite strip method of elastic buckling analysis (Hancock 1978) was used to proportion the section dimensions such that the critical stresses for distortional buckling were lower than those for local buckling for all four sections. Therefore, the intermediate slenderness columns would fail mainly in the distortional mode rather than the local mode. The dimensions of the test sections were those commonly used in the rack industry. The webs of the test sections were approximately 90 mm in depth and the flange width was in the range of 70 mm to 90 mm.

The test sections were formed from steel strips by a local rack manufacturer. The specimens of each channel section type were fabricated to the same overall dimensions but from three different material thicknesses, (namely 1.7 mm, 2.0 mm and 2.4 mm). The 1.7 mm and 2.0 mm thick steel were hot-rolled rimming steel with specified minimum yield strengths of 340 MPa and 200 MPa respectively. They have been designated as HR340 and HR2 in Australain Standard AS1594 (1981). The 2.4 mm thick steel was a cold-reduced zinc-coated steel being designated as G450 in Australian Standard AS1397 (1984) with a specified minimum yield strength of 450 MPa. The mean measured dimensions for each test section are given in Table 1.

4. MECHANICAL PROPERTIES OF THE SPECIMEN MATERIAL

Tensile and compression coupons were taken from the flat elements and corners of the test sections. The flat tensile coupons were prepared and tested according to Australian Standard AS1391 (1974). The corner tensile coupons, with the ends flattened by using a vice, were gripped in the same manner as the flat tensile coupons. The compression coupons were rectangular (90 mm × 25 mm) with all edges being milled and were tested in a greased steel jig of a similar type to that described by Karren (1967).

The tensile and compression coupons were tested in an Instron TT-KM (250 kN) testing machine using a calibrated extensometer on a 25 mm gauge length. The results of the tensile and compression coupon tests are given in Table 2 for the flat tensile coupons, the corner tensile coupons and the compression coupons. The 0.2 percent proof stress was used for all coupons since they all exhibited gradual yielding. The ratios of the proportional limit (σ_p) to yield strength (σ_Y) of the flat tensile and compression coupons were found to be in the range 0.56 to 0.68. The mean yield strengths of the corner coupons were found to be 24 percent, 61 percent and 9 percent higher than those of the flat tensile coupons for the HR340, HR2 and G450 steel respectively.

5. COLUMN TESTS

5.1 Test Configuration and Procedure

The column tests were performed in a 250 kN capacity Instron TT-KM testing machine. Due to the capacity limitation of the Instron testing machine, several of the 2.4 mm thick short columns were tested in a 2000 kN capacity Avery testing

machine. The specimen lengths selected are given in Tables 3(a)-(d) and ranged from 0.3 m to 1.9 m. The specimen designation CH17-1900, for example, refers to the 1.7 mm thick lipped channel in Fig. 2(a) with a specimen length of 1900 mm.

All test specimens were tested in a fix-ended condition. Load was applied at the top end through a rigid end platten fixed against rotation. The test specimens were seated at the bottom on a spherical bearing which was restrained from rotation about both horizontal axes and the vertical axis during testing although it was free to move prior to loading. The purpose of this bearing was to eliminate non-parallel ends prior to loading so that loading could be applied uniformly across the sections. In addition, the specimen ends were milled to provide flat loading surfaces.

Two of the test specimens, CH17-1370 and RA17-1300 had strain gauges attached on the inside and outside surfaces around their cross-sections at the mid-height position in order to measure the stress distributions in the test sections during loading.

5.2 Test Results

The failure stresses (σ_{max}), based on the maximum applied load divided by the section area, of the test specimens and their modes of buckling are given in Tables 3(a)-(d). The failure stresses were generally between the proportional limit and the yield stress of the steel from which the specimens were made. Typical distortional buckling modes of the 0.7m and 0.8m long test specimens are shown in Fig. 3. Multiple distortional buckle waves were observed in longer specimens. Flexural-torsional buckles were observed in the longest specimens. The number of distortional buckle waves given in Tables 3(a)-(d) was deduced from displacement transducer readings and from experimental observations.
The distribution of longitudinal strain for the specimens CH17-1370 and RA17-1300 as measured by the strain gauges is shown in Fig. 4. For the specimen CH17-1370, the longitudinal strain remained fairly uniform around the section until the applied load was approximately 95 percent of the maximum load attained by the specimen. For the Specimen RA17-1300, the longitudinal strain was fairly uniform in the web up to the maximum load whereas in the flanges, it was uniform up to approximately 85 percent of the maximum load.. The uniformity of the longitudinal strains measured in both specimens suggests that the loading arrangements described in the previous section performed satisfactorily in providing uniform loading at both specimen ends.

6. DESIGN RECOMMENDATIONS

6.1 General

The design specifications for cold-formed steel structures have been revised recently in the USA (AISI 1986), Europe (ECCS 1987) and Australia (Standards Association of Australia 1988). Some of the main features of the changes for the design of compression members are the adoption of a single effective width equation for both stiffened and unstiffened compression elements, and the design provisions in the AISI and ECCS for partially stiffened elements. A partially stiffened element has one longitudinal edge connected to a web element with the other longitudinal edge connected to an edge stiffener which is not of adequate size to prevent local-torsional (distortional) buckling of the section. The provisions for partially stiffened elements allow designers to calculate the plate buckling coefficient for the partially stiffened element for use in the effective

width equation. These provisions are based on the work of Desmond, Pekoz and Winter (1981) who studied the simple lip stiffener types similar to those in Figs. 2(a) and 2(d). There are no such provisions in the Australian Standard (1988). However, a rational elastic buckling analysis of the whole section, by a method such as a finite strip analysis (Hancock 1985) or the formulae in Lau and Hancock (1987), may be used to determine the plate buckling coefficients for use in the effective width equation.

There is no explicit provision for the distortional buckling mode in the AISI Specification, the ECCS Recommendations or the Australian Standard. It is considered that the existing approach of using the effective width equation may be inappropriate for the distortional buckling mode. This statement is based on the known fact that distortional buckling occurs at a much longer wavelength than local buckling and that it can occur in conjunction with local buckling. Consequently two different design approaches are described in this paper for the distortional buckling mode. The first approach accounts for distortional buckling by adjusting the effective width of the flange elements with the plate buckling coefficient based on the elastic distortional buckling stress of the section. The second approach allows designers to calculate explicitly the elastic and inelastic distortional buckling stresses of the section in a similar manner to elastic and inelastic flexural-torsional buckling.

In the following sections of this paper, the values of yield stress and Young's modulus used in the calculation of the effective widths and column curves were based on the mean compression values given in Table 2 rather than the nominal values. This allows a direct assessment of the accuracy of strength predictions in the different design specifications. The mean section dimensions given in Table 1 were used in the calculations.

6.2 Effective Width Strength Predictions

The effective width of a plate element according to the AISI, ECCS and Australian Specifications is given by the Winter formula (Winter 1968) as:

$$\frac{b_e}{b} = \left[\frac{\sigma_\ell}{f}\right]^{\frac{1}{2}}\left\{1 - 0.22\left[\frac{\sigma_\ell}{f}\right]^{\frac{1}{2}}\right\} \qquad (1)$$

$$\sigma_\ell = \frac{K \pi^2 E}{12\,(1 - \upsilon^2)}\left[\frac{t}{b}\right]^2 \qquad (2)$$

where K is the plate buckling coefficient and depends upon the support conditions, and b and b_e are the flat width and effective width respectively of the element. In the Australian Standard and the ECCS Recommendations, the value of f is taken as the yield stress F_Y while it is taken as F_n in the AISI Specification. The value of F_n is determined from the column design formula (Equations 8 and 9) and it approaches the yield stress F_Y for short columns.

The plate buckling coefficient is usually taken as 4.0 for uniformly compressed stiffened elements. For uniformly compressed unstiffened elements, the value of K is taken as 0.5 in the Australian Standard and 0.43 in the AISI Specification. The ECCS and AISI also provide equations for determining the K values for elements with edge stiffeners which are not fully effective. The equations in the AISI

Specification are similar to those in the ECCS Recommendations except that the former depend on the stress F_n while the latter depend on the yield stress. For a short length column, the K values determined using the AISI or ECCS equations will be similar because the stress F_n approaches the yield stress. The value of K for an edge stiffened element lies between 0.43 and 4.0 depending upon the adequacy of the edge stiffener.

The K values for the flanges of the test sections, as calculated using the ECCS equations and the AISI equations with the values of F_n taken as the yield stress, are given in Table 4(a) for the CH and HA sections. Since the Australian Standard permits the calculation of the K values by a rational elastic buckling analysis, finite strip analyses have been performed to determine the local buckling stresses of the CH and HA sections. The K values for the flanges determined using the finite strip buckling analysis are compared in Table 4(a) with the ECCS/AISI values.

As mentioned in Section 3, the elastic critical stresses for distortional buckling of the test sections are lower than those for local buckling. Hence the K values of the flanges of the CH and HA sections corresponding to the distortional buckling mode have also been included in Table 4(a). The K values corresponding to the distortional mode were determined from Equation 2 with σ_ℓ being replaced by the elastic distortional buckling stresses of the CH and HA sections, and b taken as the flange flat width b_f. The elastic distortional buckling stresses were determined using the finite strip analysis, although the formulae in Lau and Hancock (1987) could have been used. The K values of the flange combinations of the RA and RL sections corresponding to the distortional buckling mode are given in Table 4(b) where the flat widths b in Eq. 2 have been taken as the summation of b_1+b_2 in Fig. 2 in a manner similar to that described by Hancock (1985). In Table 4(a), the K values based on the finite strip local buckling mode are greater than those based on distortional buckling or the ECCS/AISI values while those based on the distortional buckling mode are closer to the ECCS/AISI values.

6.3 Q-factors

The Q-factor design approach has been used in the column design curves of the Australian Standard, European Recommendations and indirectly in the AISI Specification (A_e/A in Equation 7) to account for the effects of local buckling on the column strength. The Q-factor of a section is defined as the ratio of the effective section area at ultimate to the gross section area so that the product of Q and the yield stress (F_Y) gives the stub column strength. The effective area of the section is obtained by summing the effective areas of all the individual elements forming the section. According to the ECCS (and AISI), the effective area of a partial stiffener has to be reduced by multiplying by the factor I_{se}/I_{sa} (I_s/I_a in AISI).

The Q-factors have been determined by 4 different methods for comparison with the stub column strengths, and are summarised in Table 5. The four different methods used to compute Q were:

(a) In calculating the Q_1 values in accordance with the Australian Standard, the front and rear flanges of the RA and RL sections were treated as stiffened (K=4.0) and unstiffened (K=0.5) elements respectively, and the flanges of the CH and HA sections were treated as unstiffened (K=0.5).

(b) In calculating the Q_2 values in accordance with the ECCS recommendations, the front flanges of the RA sections and the front and rear flanges of the RL

sections were regarded as elements with edge stiffeners of depth d_1 and d_2 (Fig. 2) as appropriate, and the rear flanges of the RA sections were regarded as unstiffened elements. For the CH and HA sections, the K values of the flanges in Table 4(a) determined according to the ECCS equations for edge stiffened elements were used. The value of A_e/A in the AISI Specification (see Equation 7), where A_e is the effective area at the stress F_n equal to the yield stress, is equivalent to Q_2 in Table 5.

(c) In calculating the Q_3 and Q_4 values in accordance with the Australian Standard using a rational elastic buckling analysis to determine the values of K, the values of K for the flanges given in Tables 4(a) and (b) corresponding to the distortional and local modes were used. In the calculation of the Q_3 and Q_4 values for the CH and HA sections, the effective widths of the webs, flanges and stiffeners were determined separately using the appropriate K values. However, the method of calculation of the Q_3 values for the RA and RL sections was slightly different since the front and rear flanges were regarded as a single continuous element with a width of b_1+b_2, to determine an overall effective width for the combined front and rear flanges. The Q_4 values for these sections were simply taken as Q_1 since the local buckling deformations computed using the finite strip method were mainly confined to the web.

The K values of the section webs have been taken as 4.0 in the calculations for all sections.

In Table 5, the values of Q_1 are close to the values of Q_2 for the RA and RL sections since the front and rear flanges were generally fully effective as a result of their narrow widths (b_1, b_2). For the RA and RL sections, the test strengths of the stub columns agree better with the Q_1 (or Q_4) and Q_2 values while the Q_3 values are slightly conservative. For the CH and HA sections, the ECCS Q-factors (Q_2) are lower than those based on the K values of the local and distortional modes (Q_3 and Q_4) mainly as a result of the smaller K values but also as a result of the linear reduction of stiffener area as required by the ECCS Recommendations. The test stub column strengths for the CH and HA sections in general agree better with the predicted strengths based on the distortional mode (Q_3) while the ECCS predictions appear to be conservative. The predicted strengths based on the Q_1 values are very conservative for the CH and HA sections.

6.4 Inelastic Distortional Buckling

Based on the assumption of a parabolic relation between inelastic buckling stress and column slenderness ratio, Chajes, Fang and Winter (1966) derived a simple design formula for determining the inelastic buckling stress of cold-formed sections undergoing flexural-torsional buckling. A similar approach has been adopted in deriving a design formula for determining the inelastic distortional buckling stress. The proposed design formula is given by Equations 3 and 4.

$$\sigma_{di} = \sigma_{de} \qquad \text{for } \sigma_{de} \leqslant \frac{F_Y}{2} \qquad (3)$$

$$\sigma_{di} = F_Y \left[1 - \frac{F_Y}{4\,\sigma_{de}} \right] \qquad \text{for } \sigma_{de} > \frac{F_Y}{2} \qquad (4)$$

where σ_{de} and σ_{di} are the elastic and inelastic distortional buckling stresses respectively. The proposed formulae are compared in Fig. 5 with the average stress at failure (σ_{max}) of the test specimens where only those specimens which

failed by distortional buckling or whose theoretical elastic critical modes were distortional have been plotted. The theoretical elastic distortional buckling stresses (σ_{de}) of the test specimens were determined using the spline finite strip analysis (Lau and Hancock 1986) taking account of the fixed end test conditions. The proposed design formula provides a close mean fit to the test results. The elastic distortional buckling stress (σ_{de}) in Equations 3 and 4 can be determined using the design charts provided in Hancock (1985) for rack section profiles, or the approximate formulae in Lau and Hancock (1987) for channel columns which were both derived for columns with simply supported ends, provided that the columns are significantly longer than the critical half-wavelengths for distortional buckling.

6.5 Column Design Curves

The column curve in the Australian Standard (1988) is based on the Perry curve with a suitably chosen imperfection parameter. The unfactored column design curve is given by Equation 5.

$$F_m = QF_Y \left[\left[\frac{1+(1+\eta)(F_{oc}/QF_Y)}{2} \right] - \sqrt{\left[\left[\frac{1+(1+\eta)(F_{oc}/QF_Y)}{2} \right]^2 - \frac{F_{oc}}{QF_Y} \right]} \right] \quad (5)$$

where F_{oc} = elastic buckling stress

η = imperfection parameter = $(1.25-Q)QF_Y/F_{oc}$

$$Q = \frac{\text{Effective Design Area}}{\text{Full Area of the Cross-Section}}$$

The elastic buckling stress (F_{oc}) is the lesser value of the flexural or flexural-torsional buckling stress. The term (1.25-Q) in the imperfection parameter lowers the column curve as Q is reduced below 1.0 in order to allow for the interaction of local and global buckling.

The column curve in the ECCS Recommendations (1987) is also based on the Perry curve but with a different imperfection parameter from that in the Australian Standard. Using the same notation as in Equation 5, the imperfection parameter is given by Equation 6.

$$\eta = \alpha\ (4 - 3Q)\ (\sqrt{(F_Y/F_{oc})} - 0.2) \quad (6)$$

The value of α is taken as 0.34 for lipped channel sections and 0.49 for unlipped channel sections.

The unfactored column curve in the AISI Specification (1986) is based on a parabolic formula similar to that given by Equations 3 and 4 and is given by Equations 7, 8 and 9.

$$F_m = \left[\frac{A_e}{A} \right] F_n \quad (7)$$

$$F_n = F_{oc} \quad \text{for } F_{oc} \leqslant \frac{F_Y}{2} \qquad (8)$$

$$F_n = F_Y \left[1 - \frac{F_Y}{4 F_{oc}} \right] \quad \text{for } F_{oc} > \frac{F_Y}{2} \qquad (9)$$

where A_e is the effective area at the stress F_n.

6.6 Proposed Design Methods

In conjunction with the column curve in the Australian Standard (1988), two design alternatives have been proposed for the distortional buckling mode. They are:

Alternative I The column curve given by Equation 5 is used with the value of the Q factor taken equal to Q_3 corresponding to the distortional buckling mode or Q_4 in cases where local buckling occurs before distortional buckling.

Alternative II The column curve given by Equation 5 is used with the value of the Q factor taken equal to Q_4, corresponding to the local buckling mode only. A separate check on the distortional buckling strength (σ_{di}) is performed using the inelastic distortional buckling strength formulae given by Equations 3 and 4.

Alternative I can be used in conjunction with the existing Australian Standard (1988) by basing the values of the local buckling coefficient K used to determine Q_3 and Q_4 on a rational elastic buckling analysis.

7. COMPARISON OF TESTS WITH DESIGN METHODS

7.1 Proposed Design Methods

The unfactored design curves for the alternative design methods have been compared with the test results for the CH sections in Fig. 6, for the RA sections in Fig. 7, for the RL sections in Fig. 8 and for the HA sections in Fig. 9. Only the comparisons for the 1.7 mm thick sections (HR340 material) and 2.4 mm thick sections (G450 material) are given in Figs. 6 – 9. The comparisons for the 2.0 mm thick material (HR2) are given in Lau and Hancock (1988). The σ_{de} values used to calculate σ_{di} in Equations 3 and 4 have been based on a finite strip analysis ignoring end fixity. The F_{oc} values have been based on the Timoshenko (Timoshenko and Gere 1959) formula with the effective length for both flexure and torsion equal to 0.5 times the actual length.

At low column slenderness, the distortional buckling cut-offs (σ_{di}) in the second alternative are more conservative than the column curves of the first alternative. However at higher column slenderness, the second alternative provides better estimates of the column strength whilst still ensuring that distortional buckling has been allowed for in the design.

7.2 AISI and ECCS

The unfactored column design curves of the AISI (1986) and ECCS (1987) are also shown in Figs. 6 – 9. In making comparisons of the shapes of the column curves, it should be noted that different safety factors are used in the AISI and ECCS, and the ECCS is based on a limit state design philosophy. Therefore the purpose

of comparing the unfactored curves is to evaluate the ability of the different curves to model the specimen characteristics.

For the CH and HA sections, the AISI column curves are less conservative for intermediate to long column lengths than the ECCS curves. In this range, the AISI curves have a better shape than the ECCS curves when compared with the test results of the CH and HA sections. For the RA and RL sections, the AISI curves are unconservative when compared with the test results. The ECCS column curves for those sections are generally conservative for the long column specimens.

8. CONCLUSIONS

The results of channel section columns formed by brake-pressing have been described. A total of 68 channel columns of different section geometries, thicknesses and steel grades were tested under uniform compression in fix-ended condition. The sections consisted of lipped channels, hat sections and two types of channels used for industrial steel storage racks.

Detailed comparisons of the test results with the recently revised design rules of the American Iron and Steel Institute (1986), the ECCS (1987), and an Alternative I based on the Australian Standard (1988) show that:

(a) the stub column strengths predicted by all three specifications are reasonably accurate. In the case of the Australian Standard, the Q-factor (Q_3 in this paper) must be based on a buckling coefficient (K) determined from a distortional buckling analysis of the section.

(b) the column curves of the AISI are fairly accurate for the channel (CH) and hat (HA) sections, but are too high for the rack section profiles (RA and RL). This may simply be a consequence of the assumptions used to compute the effective widths of the flanges of the RA and RL sections.

(c) the column curves of the ECCS and the Australian Alternative I are very conservative for longer length columns which fail by flexural-torsional buckling.

An Alternative Method (II) has been proposed where the stub column strength for use with the design column curve is based on local buckling alone and not distortional buckling. A separate check for distortional buckling must be performed using an estimate of the elastic distortional buckling stress and a design curve to allow for the interaction of distortional buckling and yielding. This curve was proposed in the paper as the Johnston parabola (1976) and was found to produce an accurate estimate of inelastic distortional buckling.

The Alternative Design Method (II) was found to produce more accurate estimates of the flexural-torsional mode at longer column lengths and the distortional buckling mode at intermediate column lengths than the existing design methods which use a single column curve throughout the range of failure modes.

9. ACKNOWLEDGEMENTS

The authors are grateful to Colby Engineering Pty. Ltd., Brookvale, NSW, Australia, for supplying the test specimens.

10. APPENDIX I - REFERENCES

American Iron and Steel Institute, AISI (1986), Specification for the Design of Cold-Formed Steel Structural Members, Washington, DC.

Chajes, A., Fang, P.J. and Winter, G. (1966), "Torsional-Flexural Buckling, Elastic and Inelastic, of Cold-Formed Thin Walled Columns", Research Bulletin, School of Civil Engineering, Cornell University, Ithaca, New York, No. 66-1.

Desmond, T.P., Pekoz, T. and Winter, G. (1981), "Edge Stiffeners for Thin-Walled Members", Journal of the Structural Division, ASCE, Vol. 107, No. ST2, pp 329-353.

European Convention for Constructional Steelwork (ECCS), Technical Committee 7 - Working Group 7.1 - Design of Cold-Formed Steel Sheeting and Sections (1987), European Recommendations for the Design of Light Gauge Steel Members, First Edition.

Hancock, G.J. (1978), "Local, Distortional and Lateral Buckling of I-Beams", Journal of the Structural Division, ASCE, Vol. 104, No. ST11, pp 1787 - 1798.

Hancock, G.J. (1985), "Distortional Buckling of Steel Storage Rack Columns", Journal of Structural Engineering, ASCE, Vol. 111, No. 12, pp 2770-2783.

Johnston, B.G. (1976), Guide to Stability Design Criteria for Metal Structures, Third Edition, John Wiley and Sons, New York.

Karren, K.W. (1967), "Corner Properties of Cold-Formed Steel Shapes", Journal of the Structural Division, ASCE, Vol. 93, No. ST1, pp 401-432.

Lau, S.C.W. and Hancock, G.J. (1986), "Buckling of Thin Flat-Walled Structures by a Spline Finite Strip Method", Thin-Walled Structures, Vol 4. No. 4, pp 269-294.

Lau, S.C.W. and Hancock, G.J. (1987), "Distortional Buckling Formulas for Channel Columns", Journal of Structural Engineering, ASCE, Vol. 113, No. 5, pp 1063-1078.

Lau, S.C.W. and Hancock, G.J. (1988), "Strength Tests and Design Methods for Cold-Formed Channel Columns Undergoing Distortional Buckling", Research Report, School of Civil and Mining Engineering, University of Sydney, (in preparation).

Standards Association of Australia (1974), Methods for Tensile Testing of Metals, Australian Standard AS1391.

Standards Association of Australia (1981), Hot-Rolled Low Carbon Steel Plate, Sheet and Strip, Australian Standard AS1594.

Standards Association of Australia (1984), Steel Sheet and Strip - Hot-Dipped Zinc Coated or Aluminium Zinc Coated, Australian Standard AS1397.

Standards Association of Australia (1988), Cold-Formed Steel Structures Code, Australian Standard AS1538.

Timoshenko, S.P. and Gere, J.M. (1959), Theory of Elastic Stability, McGraw-Hill, New York.

Winter, G. (1968), "Thin-Walled Structures -Theoretical Solutions and Test Results", Preliminary Publications of Eighth Congress, IABSE, pp 101-112.

11. APPENDIX II - NOTATION

A	Gross section area
A_e	Effective section area
b	Flat width of compression element
b_e	Effective flat width of compression element
b_f	Flat width of flange of CH and HA sections
b_w	Web depth of test section excluding corner radii
b_1, b_2	Flat widths of front and rear flanges of RA and RL sections
CH	Simple lipped channel section
d, d_1, d_2	Depths of stiffeners of test section
E	Young's modulus
F_m	Unfactored column design stress
F_n	Unfactored stress determined from AISI column formulae
F_{oc}	Elastic buckling stress in axially loaded member
F_Y	Yield stress in design formulae
f	Stress in element computed using effective design width
HA	Hat section
I_{sa} (I_a)	Adequate value of I_{se} as defined in ECCS (AISI)
I_{se} (I_s)	Second moment of area of stiffener about its centroidal axis parallel with flange as defined in ECCS (AISI)
K	Plate buckling coefficient
L	Length of column
Q	Q factors
RA	Rack column section without additional lip stiffener
RL	Rack column section with additional lip stiffener
r	Inside corner radius of test section
t	Steel thickness or section thickness
η	Imperfection parameter in column design curve
ν	Poisson's ratio
σ_{de}, σ_{di}	Elastic and inelastic distortional buckling stresses respectively
σ_ℓ	Local buckling stress
σ_{max}	Failure stress of test specimen
σ_p	Proportional limit stress
σ_Y	Yield stress of material
σ_u	Ultimate tensile stress

Table 1 Mean Measured Test Section Dimensions

Test Section	t (mm)	b_w (mm)	b_f or b_1 (mm)	b_2 (mm)	d or d_1 (mm)	d_2 (mm)	r (mm)	Area (mm^2)
CH17	1.670	83.0	61.8		10.2		2.8	417.4
CH20	1.996	82.7	62.1		10.1		2.5	497.0
CH24	2.394	81.4	58.8		10.5		2.1	576.5
RA17	1.652	76.2	32.5	25.4	13.4		2.8	418.2
RA20	1.982	76.1	32.8	25.8	13.9		2.5	503.7
RA24	2.395	80.3	29.3	28.2	12.8		2.1	602.8
RL17	1.658	85.1	36.7	22.1	11.9	3.7	2.8	463.7
RL20	2.015	81.3	38.2	21.0	13.2	3.5	2.5	558.7
RL24	2.386	81.2	28.3	26.4	13.2	4.2	2.1	637.8
HA17	1.666	83.8	71.6		10.1		2.8	448.9
HA20	1.976	84.2	72.2		10.1		2.5	535.0
HA24	2.381	78.4	81.5		10.7		2.1	674.9

Table 2 Mean Values and Standard Deviations for Coupon Test Results

Type of Coupon	E ($\times 10^5$ MPa)	σ_p (MPa)	σ_Y (MPa)	σ_u (MPa)	Elongation (%)	$\frac{\sigma_p}{\sigma_Y}$	$\frac{\sigma_u}{\sigma_Y}$
HR340 (t = 1.7 mm)							
Tensile (Flat)	2.25 (0.09)	232.5 (25.4)	393.1 (14.3)	492.6 (10.8)	18.4 (0.5)	0.59 (0.05)	1.25 (0.02)
Tensile (Corner)	2.20 (0.21)	238.0 (19.8)	485.6 (11.0)	535.1 (5.9)	5.8 (1.3)	0.49 (0.04)	1.10 (0.02)
Compression (Flat)	1.85 (0.08)	228.8 (4.5)	406.2 (8.1)			0.56 (0.02)	
HR2 (t = 2.0 mm)							
Tensile (Flat)	2.15 (0.09)	149.8 (17.8)	220.2 (7.6)	329.4 (9.0)	26.0 (2.2)	0.68 (0.07)	1.50 (0.03
Tensile (Corner)	2.29 (0.13)	206.8 (25.0)	355.3 (9.5)	384.6 (9.0)	2.9 (0.5)	0.58 (0.07)	1.08 (0.02)
Compression (Flat)	2.05 (0.12)	145.7 (10.5)	217.0 (8.6)			0.67 (0.05)	
G450 (t = 2.4 mm)							
Tensile (Flat)	2.25 (0.07)	331.9 (14.0)	488.6 (7.7)	520.8 (6.2)	6.9 (1.0)	0.68 (0.03)	1.07 (0.01)
Tensile (Corner)	2.15 (0.22)	282.6 (22.4)	530.5 (10.0)	568.7 (9.5)	1.5 (0.4)	0.53 (0.04)	1.07 (0.01)
Compression (Flat)	2.00 (0.13)	298.7 (20.3)	478.8 (3.4)			0.62 (0.04)	

Values in brackets are standard deviations.

Table 3(a) Column Test Results - Simple Lipped Channels

Specimen	Test		Ratio	
	σ_{max} (MPa)	Mode	$\frac{\sigma_{max}}{\sigma_p}$	$\frac{\sigma_{max}}{\sigma_Y}$
CH17-300	302.1	L	1.32	0.74
-700	294.6	D (1)	1.29	0.73
-1100	260.0	D (2)	1.14	0.64
-1370	255.3	D (2)	1.12	0.63
-1640	247.9	D (3)	1.08	0.61
-1900	250.0	D (3)	1.09	0.62
CH20-300	213.0	L	1.46	0.98
-700	204.3	D (1)	1.40	0.94
-1100	189.1	FT	1.30	0.87
-1370	181.5	FT	1.25	0.84
-1900	178.7	FT	1.23	0.82
CH24-300	443.2	L	1.48	0.93
-800	402.8	D (1)	1.35	0.84
-1100	375.0	D (2)	1.26	0.78
-1500	343.2	FT	1.15	0.72
-1900	290.9	FT	0.97	0.61

L local mode
D distortional mode
FT flexural-torsional mode
σ_Y mean yield stress of flat compression coupons
σ_p mean proportional limit of flat compression coupons

Values in brackets are number of distortional buckle half-waves.

Table 3(b) Column Test Results - Rack Column Uprights

Specimen	Test		Ratio	
	σ_{max} (MPa)	Mode	$\frac{\sigma_{max}}{\sigma_p}$	$\frac{\sigma_{max}}{\sigma_Y}$
RA17-300	350.0	L	1.53	0.86
-800	320.7	D (1)	1.40	0.79
-1300	304.3	D (2)	1.33	0.75
-1500	302.2	D (3)	1.32	0.74
-1700	292.4	D (3)	1.28	0.72
-1900	289.1	D (3)	1.26	0.71
RA20-300	230.2	L	1.58	1.06
-800	208.0	D (1)	1.43	0.96
-1300	206.0	D (2)	1.41	0.95
-1500	202.8	FT	1.39	0.93
-1900	198.5	FT	1.36	0.91
RA24-300	456.0	L	1.53	0.95
-800	412.5	D (1)	1.38	0.86
-1100	382.0	D (2)	1.28	0.80
-1500	367.0	FT	1.23	0.77
-1700	367.0	FT	1.23	0.77
-1900	335.2	FT	1.12	0.70

L local mode
D distortional mode
FT flexural-torsional mode
σ_Y mean yield stress of flat compression coupons
σ_p mean proportional limit of flat compression coupons

Values in brackets are number of distortional buckle half-waves.

Table 3(c) Column Test Results - Rack Column Uprights with Additional Lip Stiffeners

Specimen	Test		Ratio	
	σ_{max} (MPa)	Mode	$\frac{\sigma_{max}}{\sigma_p}$	$\frac{\sigma_{max}}{\sigma_Y}$
RL17-300	337.0	L	1.47	0.83
-800	306.5	D (1)	1.34	0.75
-1300	288.0	D (2)	1.26	0.71
-1500	286.9	D (3)	1.25	0.71
-1700	280.4	D (3)	1.23	0.69
-1900	262.0	D (3)	1.15	0.65
RL20-300	227.9	L	1.56	1.05
-800	217.4	D (1)	1.49	1.00
-1300	204.7	FT	1.40	0.94
-1500	197.7	FT	1.36	0.91
-1700	198.8	FT	1.36	0.92
-1900	200.0	FT	1.37	0.92
RL24-300	450.0	L	1.51	0.94
-800	410.2	D (1)	1.37	0.86
-1100	393.9	D (2)	1.32	0.82
-1500	380.0	FT	1.27	0.79
-1700	354.9	FT	1.19	0.74
-1900	311.5	FT	1.04	0.65

L local mode
D distortional mode
FT flexural-torsional mode
σ_Y mean yield stress of flat compression coupons
σ_p mean proportional limit of flat compression coupons

Values in brackets are number of distortional buckle half-waves.

Table 3(d) Column Test Results - Hat Sections

Specimen	Test		Ratio	
	σ_{max} (MPa)	Mode	$\frac{\sigma_{max}}{\sigma_p}$	$\frac{\sigma_{max}}{\sigma_Y}$
HA17-300	269.1	L	1.18	0.66
-800	261.7	D (1)	1.14	0.64
-1300	246.8	D (2)	1.08	0.61
-1500	229.8	FT	1.00	0.57
-1700	221.3	FT	0.97	0.54
-1900	196.7	FT	0.86	0.48
HA20-300	214.1	L	1.47	0.99
-800	200.0	D (2)	1.37	0.92
-1300	202.6	FT	1.39	0.93
-1500	185.9	FT	1.28	0.86
-1700	171.7	FT	1.18	0.79
-1900	169.6	FT	1.16	0.78
HA24-300	406.0	L	1.36	0.85
-800	341.0	AD (1)	1.14	0.71
-1300	310.9	FT	1.04	0.65
-1700	245.7	FT	0.82	0.51
-1900	230.1	FT	0.77	0.48

L local mode
D distortional mode
AD asymmetric distortional mode
FT flexural-torsional mode
σ_Y mean yield stress of flat compression coupons
σ_p mean proportional limit of flat compression coupons

Values in brackets are number of distortional buckle half-waves.

Table 4(a) K Values of Flanges of CH and HA Sections

Test Section	K value of Flange			I_{se} (mm^4)	I_{req} (mm^4)	
	Finite Strip Analysis		ECCS AISI*		ECCS AISI*	AS1538
	Local Mode	Distortional Mode				
CH17	2.48	2.17	2.17	148	1260	513
CH20	2.49	1.87	2.02	171	628	842
CH24	2.32	1.58	1.42	231	2990	1407
HA17	3.04	2.41	2.08	143	1441	594
HA20	3.03	2.09	1.71	170	1304	969
HA24	3.62	2.00	1.73	243	5022	1958

I_{se} second moment of area of stiffener about its centroidal axis parallel with flange plate.

I_{req} required second moment of area of stiffener to ensure the flange plate behaves as a stiffened element.

* based on $F_n = F_Y$

Table 4(b) K Values of Flanges of RA and RL Sections

Test Section	K value of Flange (Finite Strip Analysis)
	Distortional Mode
RA17	2.09
RA20	1.86
RA24	1.54
RL17	2.05
RL20	1.77
RL24	1.63

Table 5 Comparison of Q-Factors

Test Section	Q-Factor				Ratio of Test Strength of Stub Column to Yield Stress
	Q_1	Q_2	Q_3	Q_4	
	K (flange) = 0.5	ECCS AISI*	K (flange) for Distortional Mode	K (flange) for Local Mode	
CH17	0.59	0.67	0.75	0.77	0.74
CH20	0.77	0.91	0.94	0.98	0.98
CH24	0.71	0.75	0.85	0.90	0.93
RA17	0.88	0.88	0.79	0.88	0.86
RA20	1.00	1.00	0.98	1.00	1.06
RA24	0.93	0.93	0.86	0.93	0.95
RL17	0.88	0.89	0.78	0.88	0.83
RL20	1.00	1.00	0.97	1.00	1.05
RL24	0.94	0.96	0.89	0.94	0.94
HA17	0.55	0.63	0.71	0.75	0.66
HA20	0.72	0.82	0.91	0.97	0.99
HA24	0.61	0.68	0.78	0.87	0.85

* based on $F_n = F_Y$

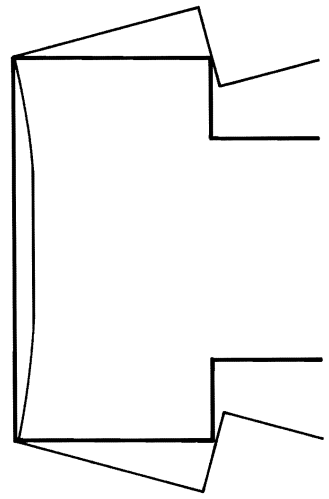

FIG.1 DISTORTIONAL MODE OF BUCKLING

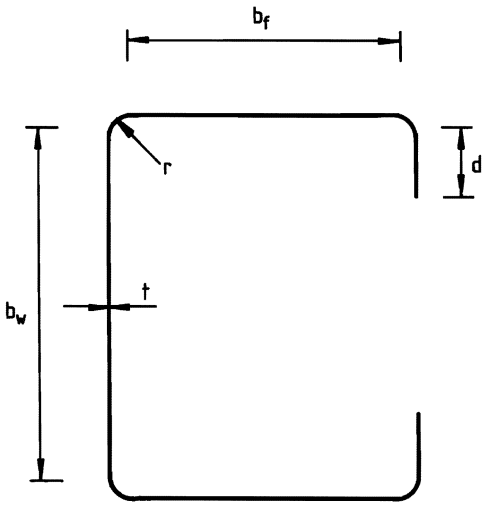

(a) Simple Lipped Channel (CH)

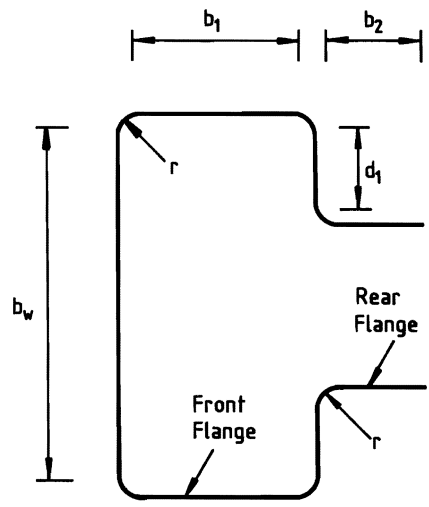

(b) Rack Column Upright (RA)

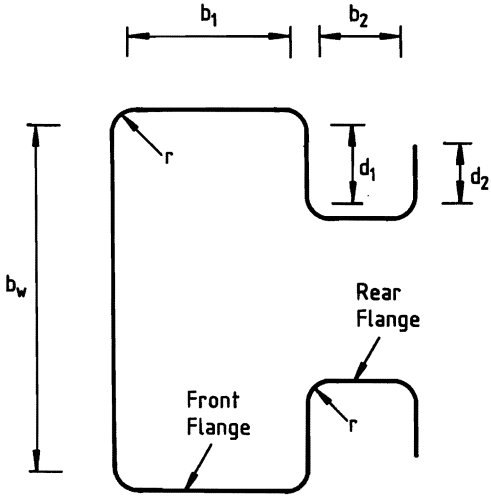

(c) Rack Column Upright With Additional Lip Stiffeners (RL)

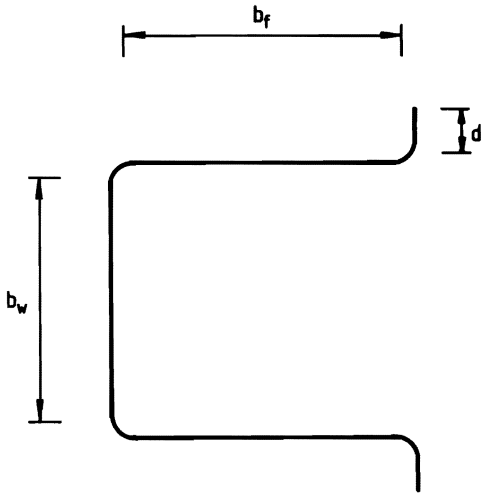

(d) Hat (HA)

FIG.2 TEST SECTIONS

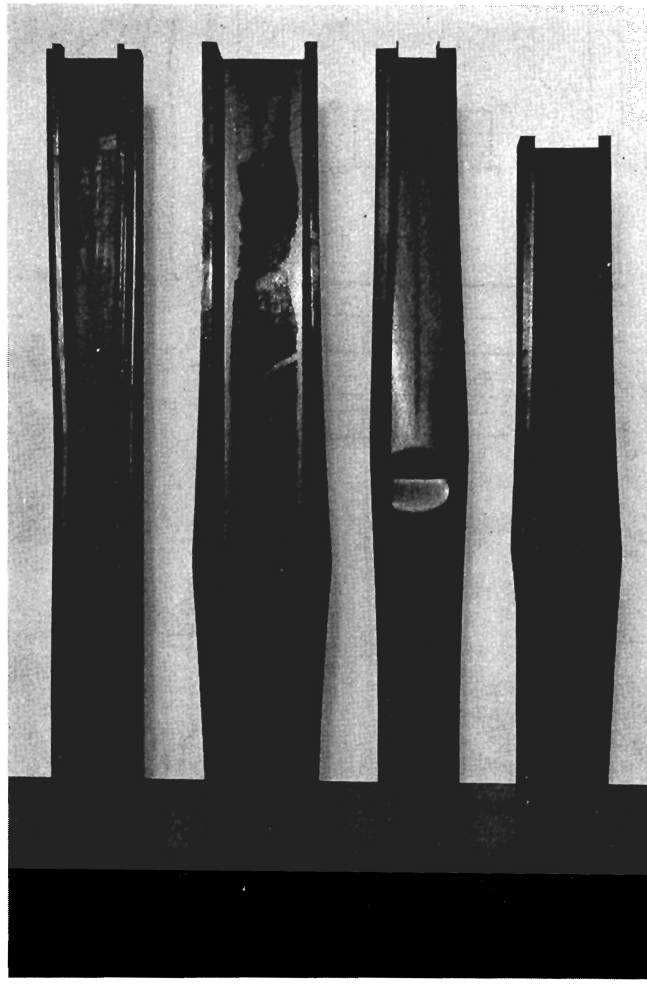

FIG.3 DISTORTIONAL BUCKLING MODES OF TEST SPECIMENS

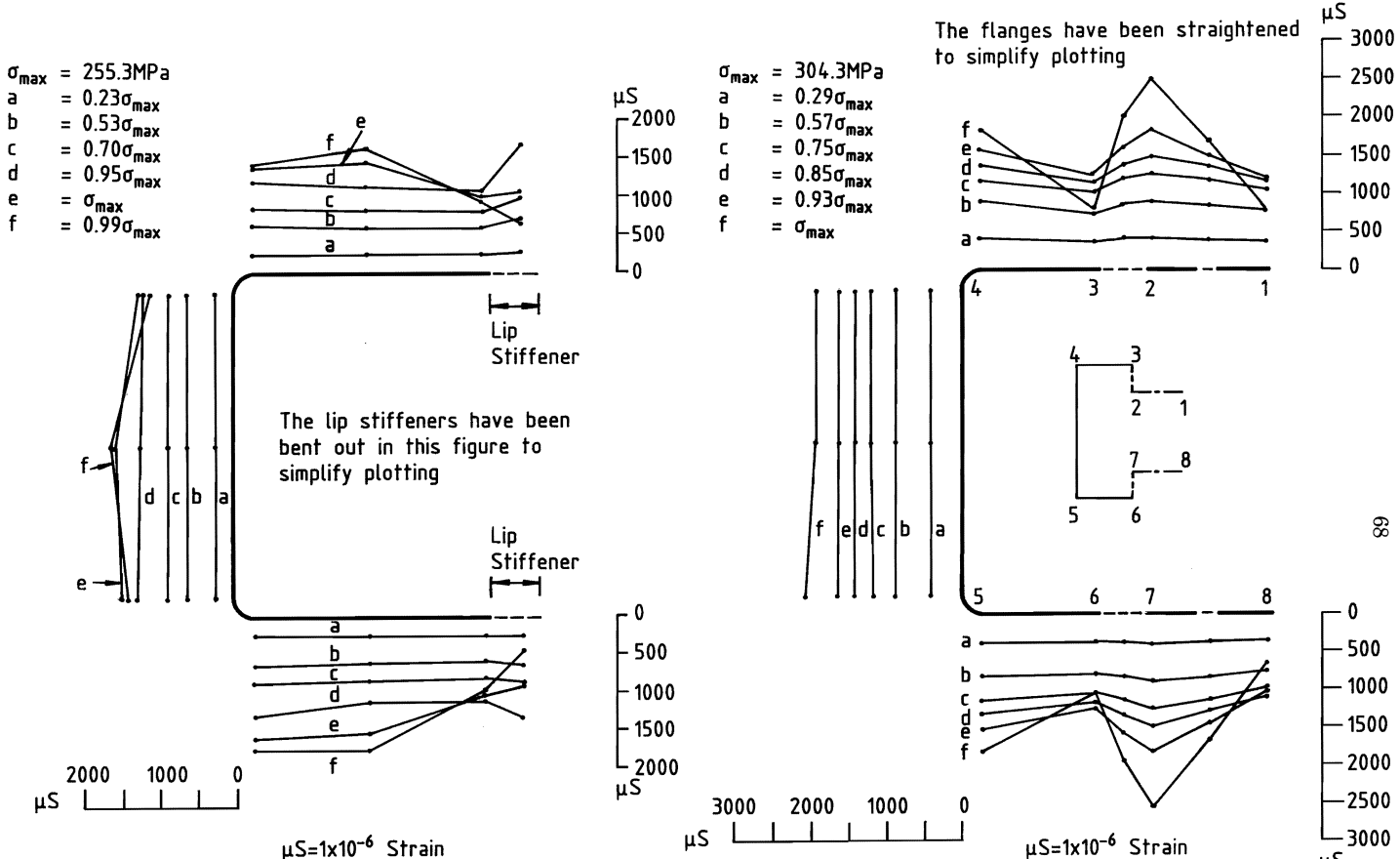

FIG.4 MEASURED LONGITUDINAL STRAIN DISTRIBUTION

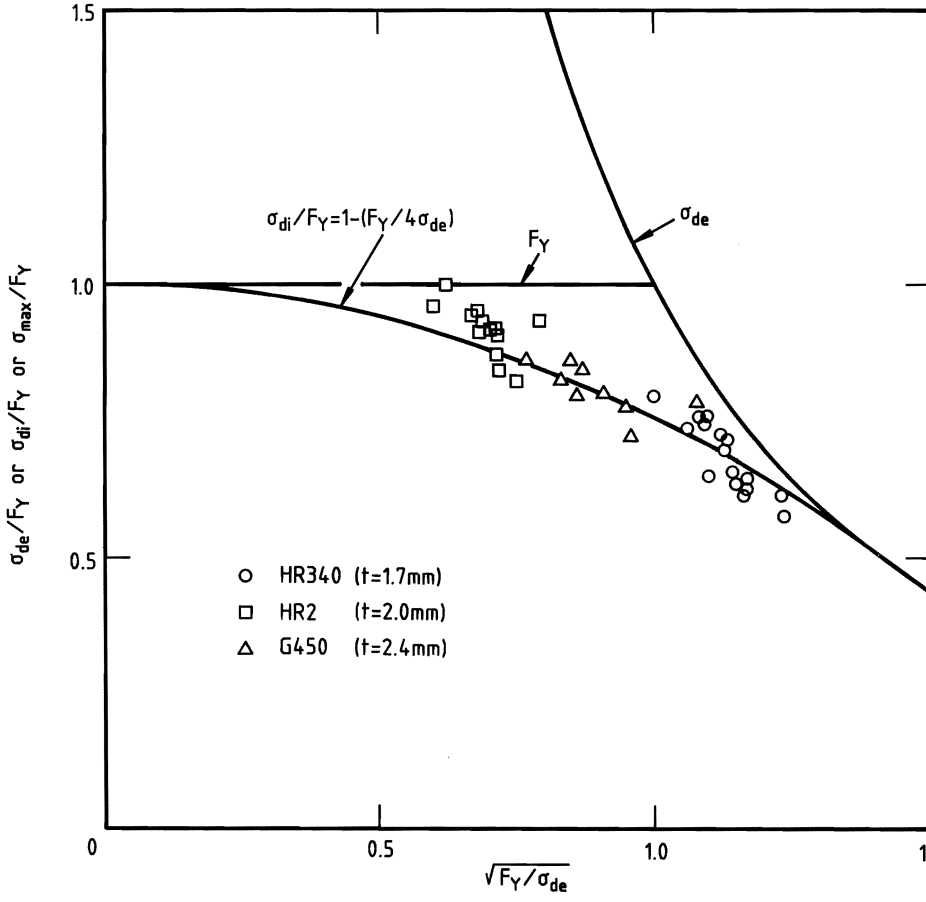

FIG.5 INELASTIC DISTORTIONAL BUCKLING FORMULA

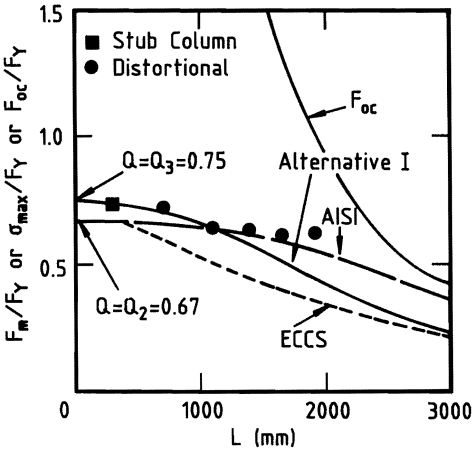

(a) Australian Alternative I, ECCS, AISI

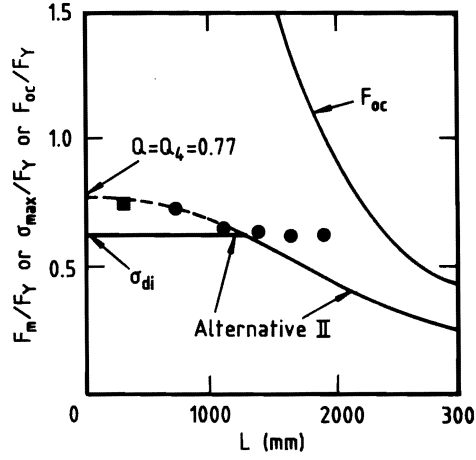

(b) Australian Alternative II

(i) CH17 (HR340 Steel)

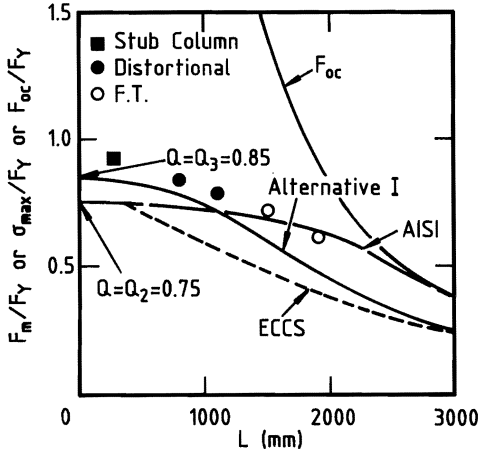

(a) Australian Alternative I, ECCS, AISI

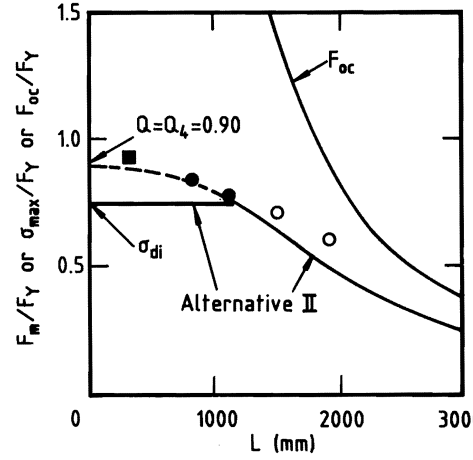

(b) Australian Alternative II

(ii) CH24 (G450 Steel)

FIG.6 COMPARISON OF PROPOSED DESIGN METHODS FOR CHANNEL SECTIONS (CH)

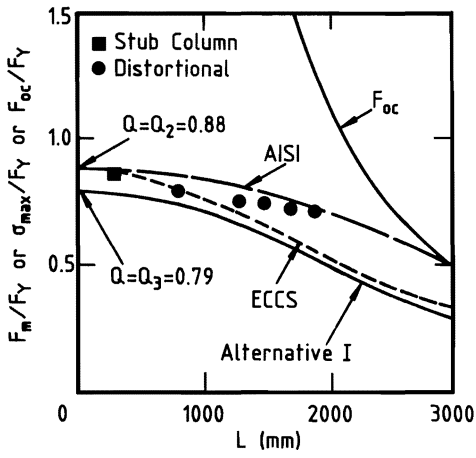

(a) Australian Alternative I, ECCS, AISI

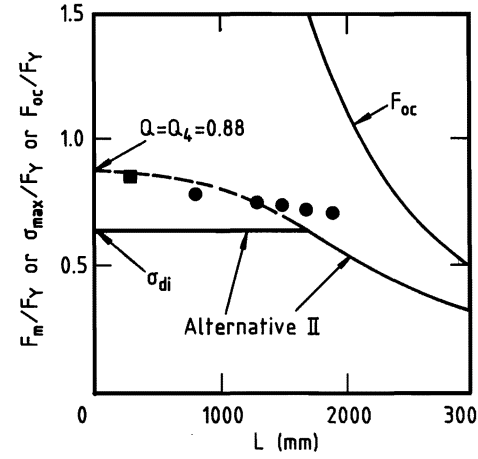

(b) Australian Alternative II

(i) RA17 (HR340 Steel)

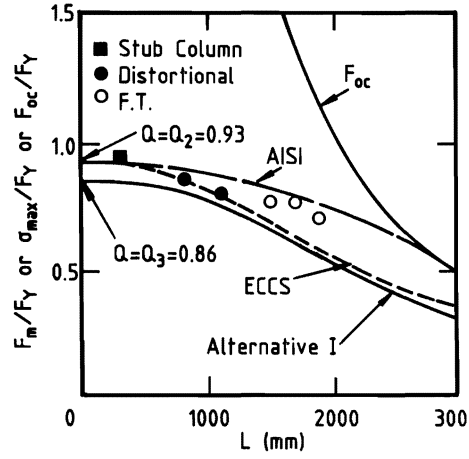

(a) Australian Alternative I, ECCS, AISI

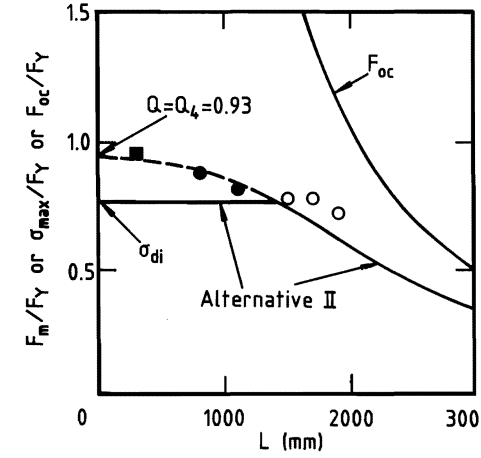

(b) Australian Alternative II

(ii) RA24 (G450 Steel)

FIG.7 COMPARISON OF PROPOSED DESIGN METHODS FOR RACK SECTIONS (RA)

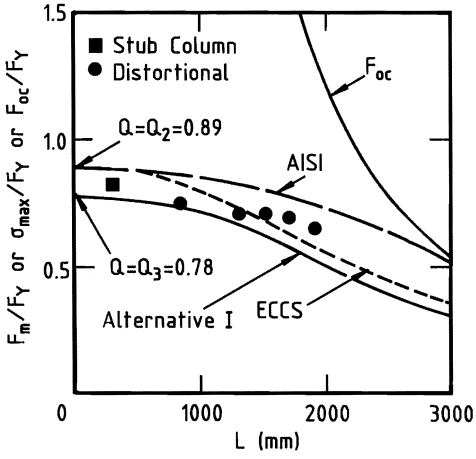

(a) Australian Alternative I, ECCS, AISI

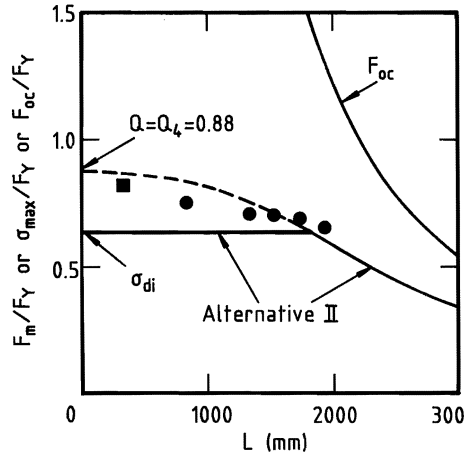

(b) Australian Alternative II

(i) RL17 (HR340 Steel)

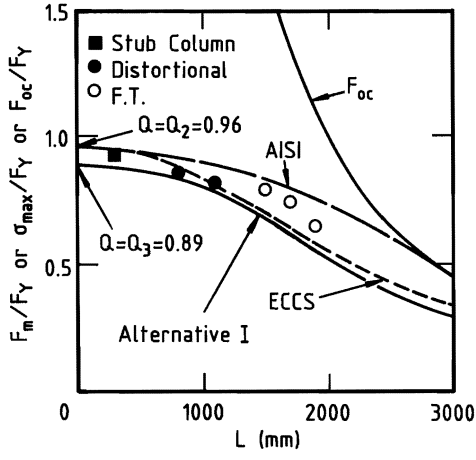

(a) Australian Alternative I, ECCS, AISI

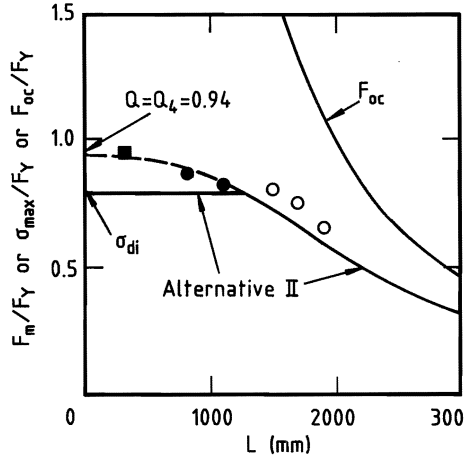

(b) Australian Alternative II

(ii) RL24 (G450 Steel)

FIG.8 COMPARISON OF PROPOSED DESIGN METHODS FOR RACK SECTIONS (RL)

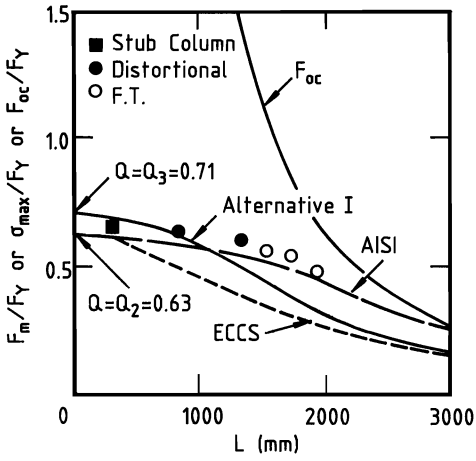

(a) Australian Alternative I, ECCS, AISI

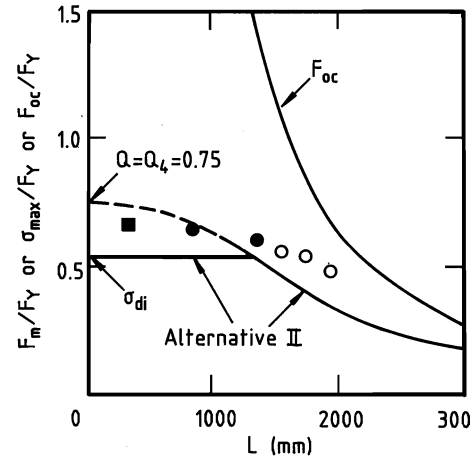

(b) Australian Alternative II

(i) HA17 (HR340 Steel)

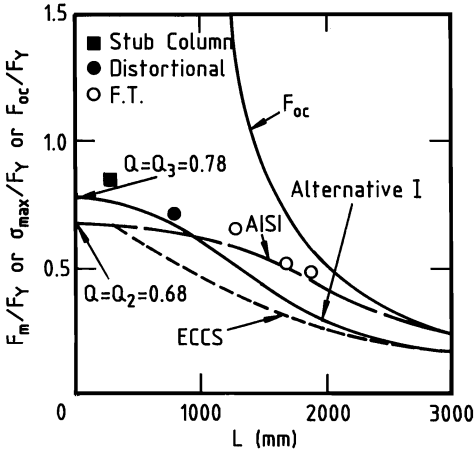

(a) Australian Alternative I, ECCS, AISI

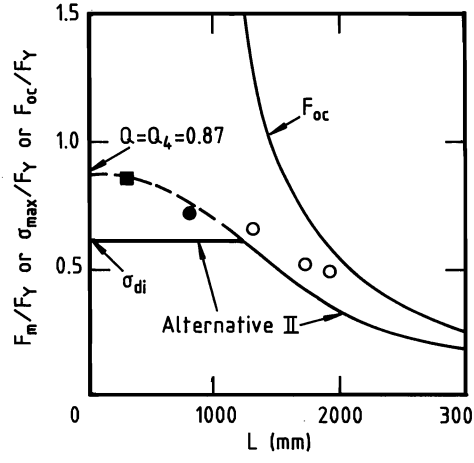

(b) Australian Alternative II

(ii) HA24 (G450 Steel)

FIG.9 COMPARISON OF PROPOSED DESIGN METHODS FOR HAT SECTIONS (HA)